Orthodontics & Craniofacial Research

ORIGINAL ARTICLE

J. Guo
Q. Wang
D. Wai
Q. Z. Zhang
S. H. Shi
A. D. Le
S. T. Shi
S. L.-K. Yen

Visible red and infrared light alters gene expression in human marrow stromal fibroblast cells

Authors' affiliations:
J. Guo, Q. Wang, Q. Z. Zhang, S. H. Shi, A. D. Le, S. T. Shi, S. L.-K. Yen, Center for Craniofacial Molecular Biology, Ostrow School of Dentistry, University of Southern California, Los Angeles, CA, USA
J. Guo, Department of Orthodontics, School of Stomatology, Shandong University, Jinan, China
Q. Wang, Guangdong Provincial Stomatological Hospital, Guangzhou, China
D. Wai, Center for Personalized Medicine, Children's Hospital Los Angeles, University of Southern California, Los Angeles, CA, USA
Q. Z. Zhang, A. D. Le, Department of Oral and Maxillofacial Surgery, School of Dental Medicine, University of Pennsylvania, Philadelphia, PA, USA

Correspondence to:
Dr. Stephen L.-K. Yen
Center for Craniofacial Molecular Biology
Ostrow School of Dentistry
University of Southern California
CSA 103, 2250 Alcazar St.
Los Angeles, CA 90033
USA
E-mail: syen@usc.edu

Date:
Accepted 16 November 2014

DOI: 10.1111/ocr.12081

Guo J., Wang Q., Wai D., Zhang Q. Z., Shi S. H., Le A. D., Shi S. T., Yen S. L.-K. Visible red and infrared light alters gene expression in human marrow stromal fibroblast cells
Orthod Craniofac Res 2015; **18**(Suppl.1): 50–61. © 2015 John Wiley & Sons A/S. Published by John Wiley & Sons Ltd

Structured Abstract

Objectives – This study tested whether or not gene expression in human marrow stromal fibroblast (MSF) cells depends on light wavelength and energy density.

Materials and Methods – Primary cultures of isolated human bone marrow stem cells (hBMSC) were exposed to visible red (VR, 633 nm) and infrared (IR, 830 nm) radiation wavelengths from a light emitting diode (LED) over a range of energy densities (0.5, 1.0, 1.5, and 2.0 Joules/cm^2) Cultured cells were assayed for cell proliferation, osteogenic potential, adipogenesis, mRNA and protein content. mRNA was analyzed by microarray and compared among different wavelengths and energy densities. Mesenchymal and epithelial cell responses were compared to determine whether responses were cell type specific. Protein array analysis was used to further analyze key pathways identified by microarrays.

Result – Different wavelengths and energy densities produced unique sets of genes identified by microarray analysis. Pathway analysis pointed to TGF-beta 1 in the visible red and Akt 1 in the infrared wavelengths as key pathways to study. TGF-beta protein arrays suggested switching from canonical to non-canonical TGF-beta pathways with increases to longer IR wavelengths. Microarrays suggest RANKL and MMP 10 followed IR energy density dose–response curves. Epithelial and mesenchymal cells respond differently to stimulation by light suggesting cell type-specific response is possible.

Conclusions – These studies demonstrate differential gene expression with different wavelengths, energy densities and cell types. These differences

in gene expression have the potential to be exploited for therapeutic purposes and can help explain contradictory results in the literature when wavelengths, energy densities and cell types differ.

Key words: Akt 1; infrared; low-level laser treatment; mesenchymal stem cell; microarray; OPG; protein array; RANKL; TGF-beta

Introduction

Visible red (VR) and infrared (IR) wavelengths have been used to treat pain (1) as well as bone and muscle injury (2, 3). In dentistry, new applications include accelerated osseointegration of implants (4) and accelerated orthodontic tooth movement (5). The devices for light therapy are considered safe as many devices have FDA approval, yet the efficacy and mechanism of action are not well understood. For example, the literature contains contradictory outcomes with different wavelengths and energy densities (6). As VR and IR light can penetrate soft tissues and bone, light treatment known as low-level laser treatment (LLLT) is an attractive non-invasive method for delivering a biological activator that can target tissue in a dose-specific manner. In bone, several studies demonstrated that LLLT can accelerate fracture healing by facilitating angiogenesis (7) and by promoting higher bone cell proliferation (8) at the fracture site. These studies present a model for accelerated bone turnover which can be potentially exploited for orthodontic tooth movement. A recent randomized clinical trial using continuous light at a wavelength of 850 nm (9) showed a significant increase in the rate of early alignment tooth movement. To date, it has been difficult to compare the results from clinical and basic science studies because each study tended to focus on one particular wavelength and energy density which often differed from other studies. Without a comparison of a range of experimental conditions, it remains difficult to optimize the conditions for a particular clinical application.

This study was developed to systematically investigate two frequently used wavelengths of light, 633 nm in the visible red region and 830 nm in the infrared region, at four energy densities in a cell culture model. The strategy was to test whether LLLT could produce effects on gene expression and cell proliferation and to look for patterns in the biological outcomes for these two parameters. Our strategy used microarrays and protein arrays, in addition to candidate gene approaches, to search for possible genes and gene networks that were activated by light. It was recognized that the response of a cell might involve multiple interdependent pathways. Given the controversy among the published studies, it was not clear whether any cell response or change in gene expression would be reproducible or would follow a pattern. Underlying this study was a hypothesis that the clinical effects of LLLT stimulation of cells are produced by altered gene expression when compared to unlit control cells. To simplify experiments and minimize effects of repeated treatments, cells were stimulated once in a non-pulsed manner and examined at a later time point when cells would be expected to undergo differentiation.

Materials and methods

hBMSC isolation and culture

Commercially available human bone marrow aspirates from two healthy adult donors were purchased from AllCells (Emeryville, CA). Human bone marrow stem cells (HBMSCs) were isolated from the aspirates following published protocols(10, 11) and then cultured in α-MEM supplemented with 10% FBS, 100 μM L-ascorbic acid-2-phosphate, 2 Mm L-glutamine, 100 U/ml penicillin, and 100 μg/ml streptomycin as reported previously, at 37°C in a humidified tissue culture incubator with 5% CO_2. The medium was changed 2 or 3 times every week, and

cells from the third passages were used for assays.

NHEK-Neo culture

Neonatal normal human epidermal keratinocytes were purchased from Lonza (Walkerville, MD), seeded at 3500 cells/cm in either serum-free KGM-Gold (keratinocytes growth medium) per manufacturer's specifications or with 10% fetal bovine serum. All cultures were incubated with EpiLife keratinocyte supplement (Life technologies) 1 μg/ml gentamycin sulfate and 2.5 μg/ml amphotericin B at 37°C in a humidified tissue culture incubator with 5% CO_2. The medium was changed every 2–3 days and tested at 40% confluence.

Capacity for multipotent differentiation of isolated hBMSC

To induce osteogenic differentiation, hBMSCs were seeded into 6-well plates at a density of 2×10^5 cells/well in MSC growth medium. The medium was replaced with osteodifferentiation-inducing medium (200 ml complete culture medium containing 1 mM dexamethasone, 500 nM isobutylmethylxanthine and 50 mM indomethacin) after 24 h adherence. After 4 weeks, bone mineralization was assayed and quantified using Alizarin red staining.

Adipogenic differentiation

hBMSCs were cultured in adipogenesis-inducing medium supplemented (Lonza, Walkerville, MD) with 1 mM dexamethasone, 500 nM isobutylmethylxanthine and 50 mM indomethacin and the differentiated adipocytes were identified and quantified by Oil Red O staining.

LED irradiation

To test a range of energy densities, arrays of light emitting diodes (LEDs) that emitted 633 nm visible red (VR) and 830 nm infrared (IR) wavelengths were custom-built and used to produce even illumination of culture wells. The light energy output was measured with a laser meter (Ophir Laser Power/Energy Meter, Jerusalem, Israel). Immediately after media changes, the hBMSCs in the test groups were exposed to LED irradiation for different exposure times to produce energy densities of 0.5, 1.0, 1.5, and 2.0 Joules/cm^2 (Table 1). All assays were run in duplicate and compared with an unlit control group under identical culture conditions. The cells were subsequently placed in osteogenic media for BrdU, Western blot, and microarray assays (Fig. 1).

Table 1. **Different experimental conditions comparing light at 830 nm and 633 nm at four energy densities against unlit control cultures.**

	Light energy (Joules/cm square)		
	Light	J/cm^2	Wavelength
C	None	0	No light
I–0.5	Infrared	0.5	830 nm
I–1.0	Infrared	1.0	
I–1.5	Infrared	1.5	
I–2.0	Infrared	2.0	
R-0.5	Visible red	0.5	633 nm
R-1.0	Visible red	1.0	
R-1.5	Visible red	1.5	
R-2.0	Visible red	2.0	

BrdU staining

After light irradiation, hBMSCs were cultured for 60 h and cell proliferation was measured using BrdU (bromodeoxyuridine) labeling and direct cell counts (7). Cultured cells were exposed to 1 M BrdU in the culture medium for 2 h at 37°C, then washed twice with 0.1 M PBS, fixed in 90% ethanol for 10 min, and washed in PBS. The fixed cells were incubated with anti-BrdU monoclonal antibody (1:100 dilution) for 1 h at room temperature, washed in PBS, and incubated with fluorescein-conjugated goat anti-mouse immunoglobulin G (IgG, 1:40 dilution) for 1 h. To confirm the presence of cells, the specimens were washed three times with cytoskeleton-stabilizing (CS) buffer and incubated for 30 min at 4°C with tetramethyl rhodamine isothiocyanate (TRITC) phalloidin (Molecular

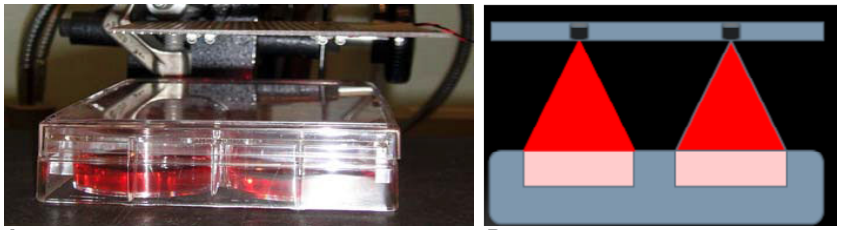

Fig. 1. Custom LED array for even illumination of cell cultures (A) Photograph of array and culture plates. (B) Schematic illustration. Culture plates (six well, Life Technologies, Grand Island, NY) were removed from culture incubators and exposed to light in a sterile hood at fixed distances. Energy density varied according to time of light exposure based on calculations by P Matthews. Power density was confirmed with laser meter (Ophir, Jerusalem, Israel).

Probes, Eugene, OR; 1:40 dilution). After three additional washes in 0.1 M PBS, the cells were enclosed with glycerol–PBS solution containing 1,4-diazabicyclo [2.2.2] octane (Sigma, 100 mg/ml) to prevent fluorescence decay.

The samples were examined using a fluorescence microscope (Olympus Optical, Tokyo, Japan), and the proliferation rate (BrdU-positive cells per phalloidin-positive cells) was calculated in 10 randomly selected fields for each of the two samples.

Human gene ST arrays

RNA was isolated (Qiagen, Santa Clara, CA) from duplicate cultures collected after 14 days post-illumination. At the Children's Hospital Los Angeles/USC Microarray Core facility, the mRNA was reverse transcribed and assayed for RNA integrity, using 5′ and 3′ probes, and analyzed using Human Exon 1.0ST arrays (Affymetrix, Santa Clara, CA) containing 1.4 million probe sets covering 32 020 coding transcripts with 40 probes per gene. Computation analysis of the exon expression profile and pathway analysis for illuminated and unlit control conditions utilized a twofold screen (Ingenuity pathway analysis, Redwood City, CA and Partek Inc., St. Louis, MO).

Quantitative RT-PCR analysis

To confirm energy density dose–response patterns in the microarray data, RNA was extracted from the cell cultures using Trizol reagent (Invitrogen, Carlsbad, CA) according to the manufacturer's protocol. The RNA was digested with DNase to eliminate any contamination from genomic DNA before performing quantitative RT-PCR. After DNase treatment, the RNA was purified using RNeasy Plus Mini Kits (Qiagen, Valencia, CA). Quantitative PCR was performed by Qiagen qPCR services (SA Biosciences, Valencia, CA) using proprietary PCR sequences and SYBR green/probe/multiplex detection with a Rotor-Gene Q cycler for genes encoding IL-1a, MMP10, glyceraldehydes-3-phosphate dehydrogenase (GADPH) and β-actin.

Antibody array: protein expression profiling

Based on mRNA microarray analyses, certain pathways and extracellular matrix proteins were predicted to show differences in expression among the different combinations of wavelengths and energy densities. Proteins were extracted and analyzed using the Explorer antibody array (Full Moon Biosystems, Sunnyvale, CA), which contained 656 antibodies for proteins produced from nine biochemical pathways. This array was used to compare proteins produced by control cells and cell cultures exposed to IR or VR light at energy densities of 0.5 and 2.0 Joules/cm^2. The Explorer array was used to confirm the changes in extracellular proteins observed in the cultures exposed to 2.0 Joules/cm. A TGF-beta array with 176 highly specific and well-characterized phosphorylated and non-phosphorylated antibodies was used to analyze TGF-beta signaling patterns in proteins from control cells and cultured cells exposed to IR and VR light at an energy density of 0.5 Joules/

cm^2. Antibody arrays were performed in five replicates. The TGF-beta antibody array was used to confirm switches that occurred in TGF-beta signaling in cells exposed to VR and IR light.

Mesenchymal vs. epithelial cell comparison

Both serum and serum-free conditions were used to compare hBMSC and NHEK-Neo cultures 1 day following IR and VR light exposures at energy densities of 0.5 and 2.0 Joules/cm^2. All groups were compared with control cell cultures. mRNA was extracted as described above for use with HuEx 1.0 ST arrays (Affymetrix, Santa Clara, CA) and analyzed using Partek and Ingenuity softwares (Ingenuity pathway analysis, Redwood City, CA and Partek Inc.).

Results

IR light produces differences in cell proliferation

All mesenchymal cell cultures were positive for bone formation and for adipocyte cell differentiation**.** Clear differences in cell proliferation were observed between control cell cultures and cells exposed to IR light at particular energy densities. A maximum of 40% change was observed in BrdU staining consequent to exposure to IR light at an energy density of 0.5 J/cm^2 (Fig. 2).

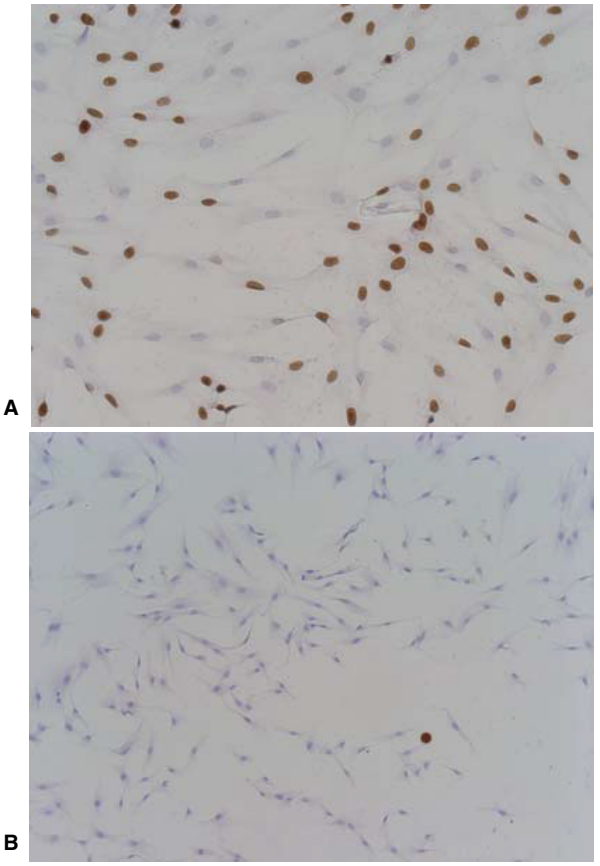

Fig. 2. Test of light effects on cell proliferation. BrdU staining of (A) illuminated (visible red 0.5 Joules/cm^2) vs. (B) unlit control hBMSC cell cultures. Human bone marrow primary cell culture were seeded at the same initial cell density and then manually counted at 12-h time points for 60 h when the cultures were assayed for BrdU labeling.

Different wavelengths and energy densities produce different profiles of gene expression

A microarray assay was performed using a two-fold (2×) screen to analyze the effect of LLLT on the expression of all the exon genes in RNA isolated from cells of the eight different test conditions and additional control group. Table 2 illustrates the range of responses to different conditions of light exposure. Each experimental condition produced a unique set of expressed genes that varied in number. Depending on the wavelength and energy density, the number of genes with expression levels two times above or below control cells varied from four genes to 1900 genes. Figure 3 shows that the 2 × screen analysis identified uniquely expressed genes as well as genes with overlapping expression following exposure of cells to IR and VR light. Of 418 genes and 2612 genes deregulated by IR and VR light, respectively, there were an additional 292 genes that were deregulated by both IR and VR wavelengths. For each wavelength,

Table 2. **ANOVA identified the above number of significantly deregulated genes vs. control ($P < 0.05$ with false discovery rate correction)**

Energy density (J/cm^2)	Infrared	Visible red
0.5	299	1210
1.0	7	27
1.5	166	4
2.0	24	1900
Total	418	2612

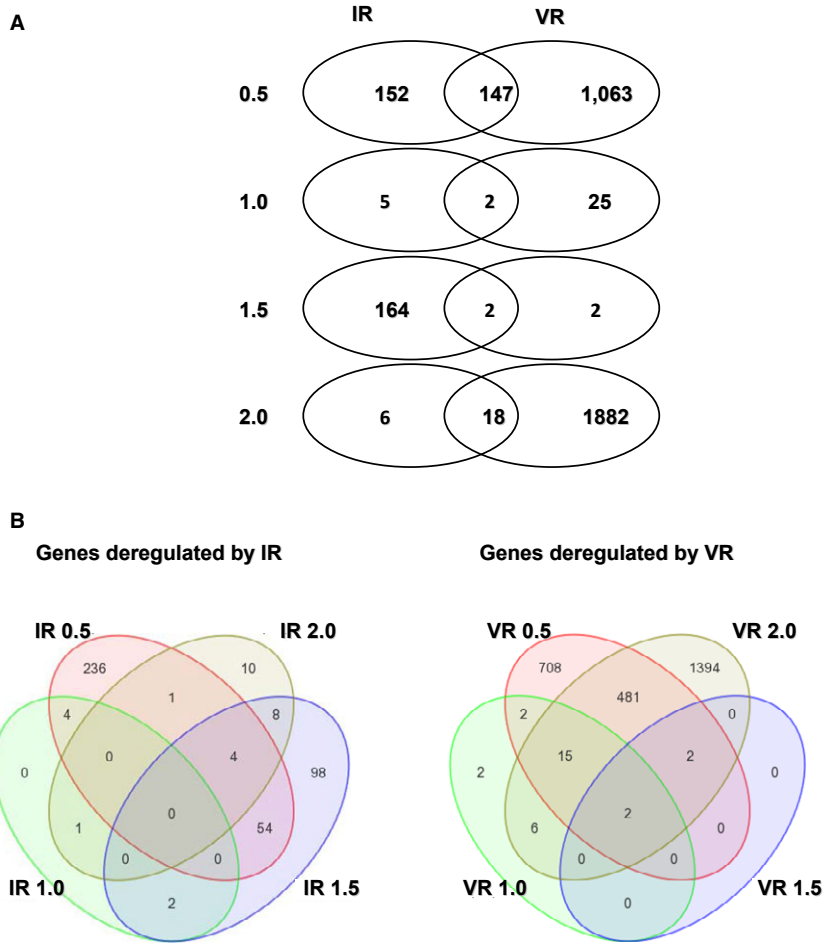

Fig. 3. (A) Venn diagram comparing two wavelengths of light: IR—infrared (830 nm), and VR—visible red (633 nm) at four energy densities ranging from 0.5 to 2.0 J/cm^2 (B) Three-dimensional Venn diagram showing overlap among the four energy densities (0.5, 1.0, 1.5, and 2.0; J/cm^2) for 830 nm (IR—infrared) and 633 nm (VR—visible red) wavelengths of light.

among the four different energy densities tested, there was vertical overlap of gene deregulation. With respect to genes deregulated by both IR and VR, some of these shared genes showed dose–response curves. Figure 4 shows candidate genes reported to be involved in the early stage of tooth movement and are associated with regulation of bone resorption. Levels of mRNA encoding RANKL and MMP 10 increased in a dose-dependent manner with increasing energy in the infrared red (830 nm) but not in the VR wavelength (633 nm). OPG, the RANKL decoy receptor/inhibitor did not change in mRNA content when RANKL mRNA was increasing with increased energy density. Similarly, the level of mRNA for TIMP1, an MMP inhibitor, did not change while MMP10 mRNA expression increased in a dose-dependent manner in the IR wavelength. These patterns did not occur under exposure to light in the VR wavelength. Ingenuity and Partek bioinformatic softwares were used to identify the top gene networks associated with each wavelength. The top gene networks for visible red light were associated with skeletal and muscular system development and function, tissue development, and amino acid metabolism. These gene networks regulate bone turnover. With respect to infrared light, the top gene networks identified were associated with cancer, skin diseases, genetic disorders, and immune diseases. The pathway analysis for visible red (633 nm) light was mapped (Fig. 5) and resulted in a convergence of pathways at TGF-beta 1. In contrast, the pathway mapped for infrared (830 nm) light showed no TGF-beta 1 convergence, and the appearance of a new pathway node through Akt 1 via the phosphoinositide 3-kinase (P13K) complex. In summary, the mRNA microarray pathway analysis pointed to two pathways, with a TGF-beta 1 response to visible red light and an Akt 1 response to infrared light.

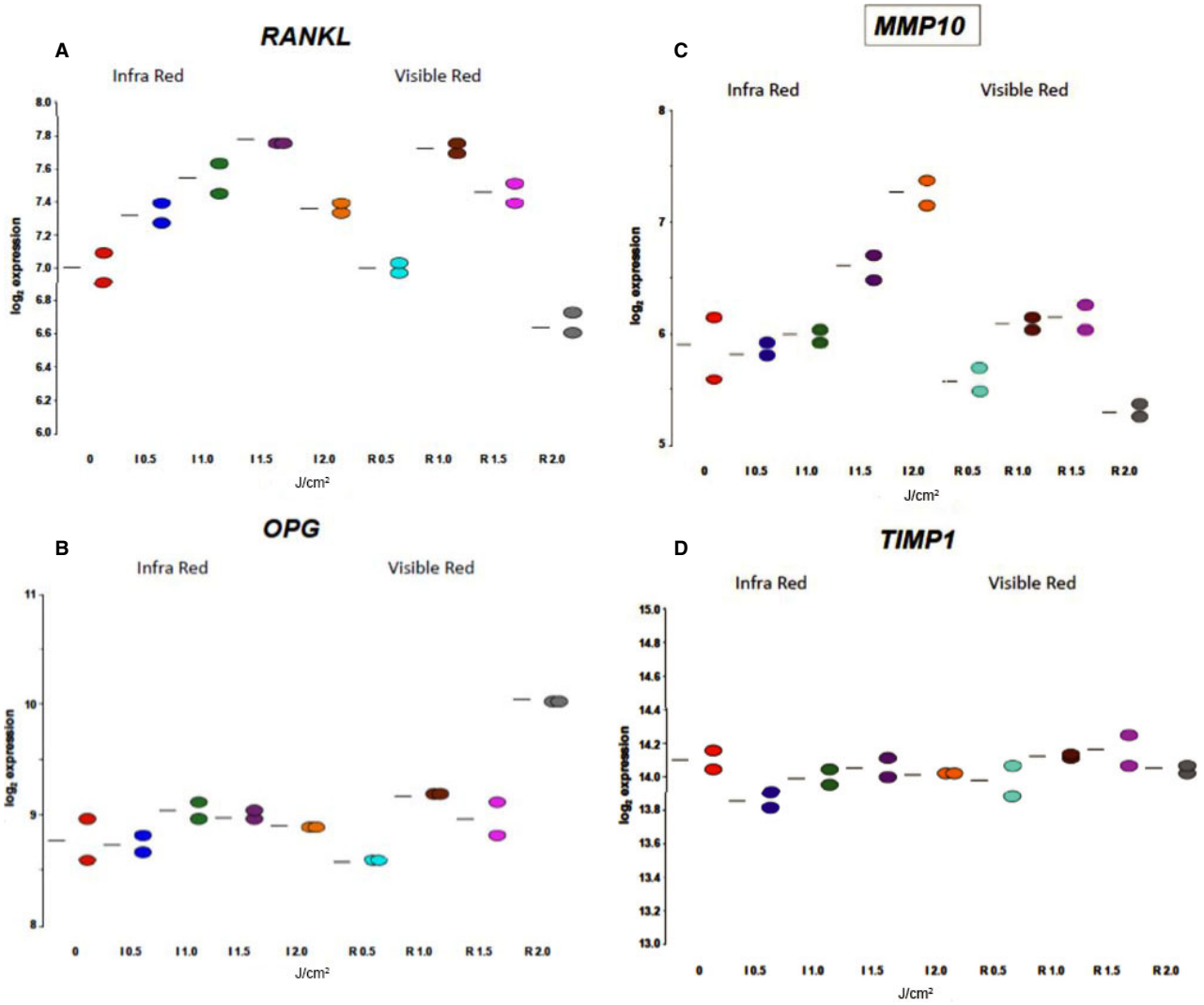

Fig. 4. Microarray analysis of candidate genes: (A) RANKL, (B) OPG, (C) MMP10, and (D) TIMP

Differential effects of visible and infrared light on canonical and non-canonical TGF-beta 1 pathways

To confirm whether the changes in mRNA content were translated into similar changes in protein content, protein arrays were performed on cell samples exposed to the lowest and highest energy densities for each wavelength as these conditions produced the greatest differences in gene expression. Figures 5 shows that visible red light exposure was associated with an upregulation of TGF-beta 1 and TGF-beta 3, but not TGF-beta 2 (Fig. 6A), and an upregulation of TGF-beta receptors 1 and 2 (Fig. 6A) and of Smad1 and Smad2 (Fig. 6B). The TGF-beta array also detected increased phosphoserine 179 of Smad3 and phosphothreonine 220 of Smad2. Additionally, there was a less than twofold increase in phosphoserine 187 of Smad1. This canonical TGF-beta 1 response was reversed with exposure to 830 nm infrared light and was replaced with an upregulation of the non-canonical TGF-beta components SEK1/MMK4, JNK, PAK1, PAK2, and PAK3, and Rho/RacGNEF (Fig. 6C). The maximum differences in TGF-beta 1 proteins following exposure to visible or infrared light occurred at lowest energy density of 0.5 J/cm^2 (Fig. 6A, C).

Protein array profiles changes in expression of oncogene, c-Myc, Akt 1 pathway components, and extracellular matrix genes with exposure to infrared light

Based on the microarray pathway map predicting the involvement of Akt 1, an Explorer

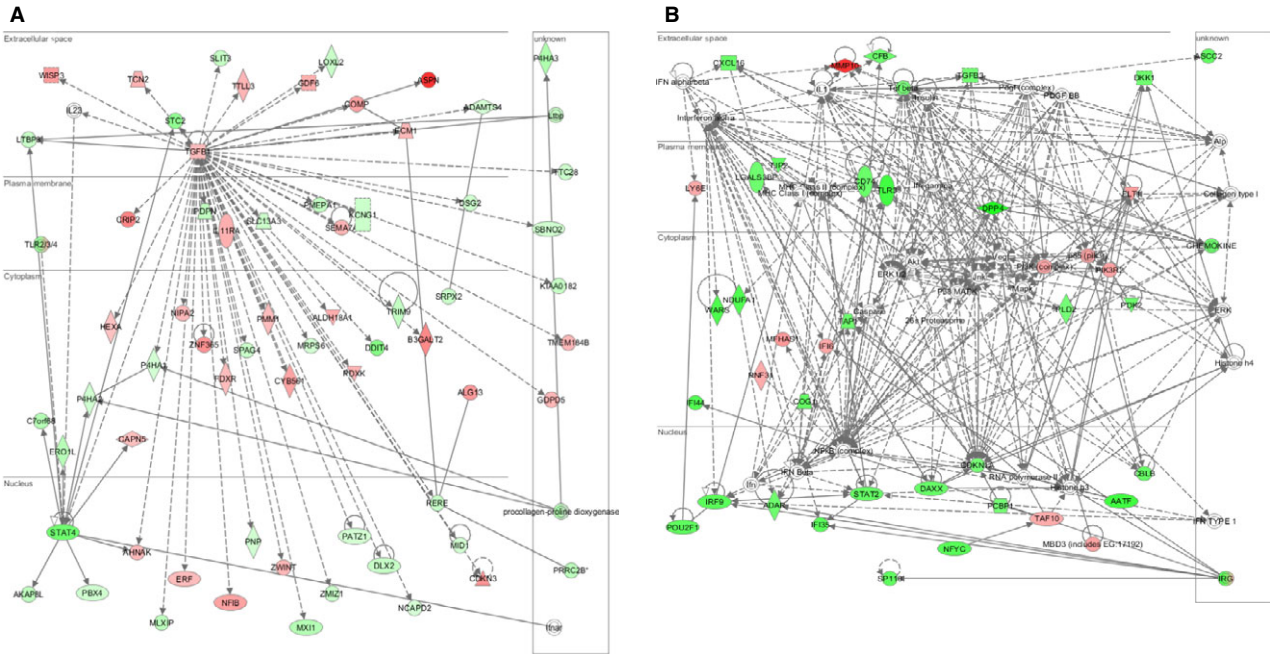

Fig. 5. Pathway analysis illustrating (A) convergence of TGF-beta 1 in VR and (B) emergence of Akt 1 pathways in IR networks. The 126 IR genes and 2320 VR genes were uploaded into Ingenuity Systems Pathway Analysis 9.0. Red = upregulation; green = downregulation

protein array was used to examine this pathway as well as other response-related proteins. The protein arrays (Fig. 6D) showed an upregulation of Akt 1 and PP2a with infrared light exposure. With IR wavelengths, the protein arrays also detected an increase in Akt 1 phosphorylated serine 124, serine 246 and threonine 450, phosphorylated mTOR threonine 2446. The predominant pathway at 633 nm was the TGF-beta 1 pathway whereas at 830 nm, it was the Akt 1 pathway. In addition, there was an upregulation of c-myc (Fig. 6B). There was also an increase in proteins that potentially are involved in controlling an inflammatory response, the cytokines cd51, cd37, cd63, and cd84, and in the late tissue repair alkaline

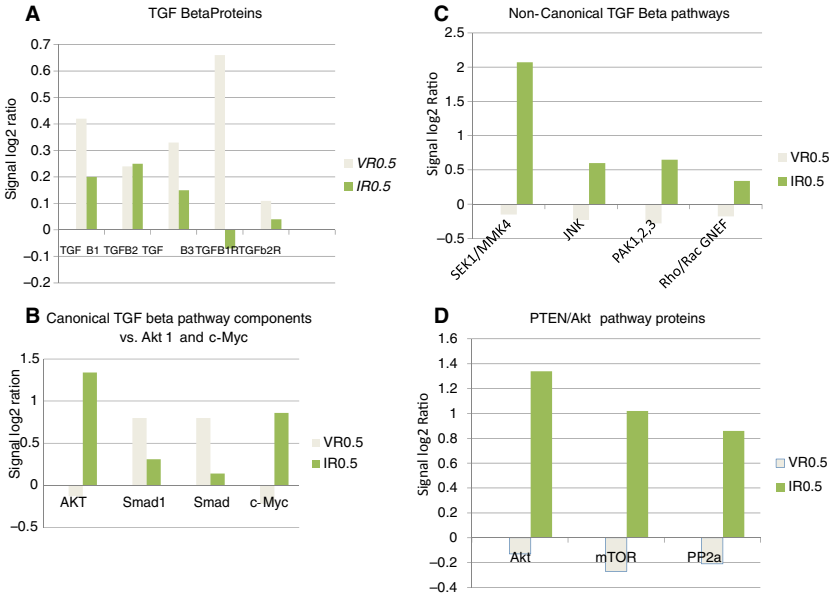

Fig. 6. A-D: Protein array data illustrating components of pathways involving TGF-beta, Akt 1 and related proteins. The *y*-axis is the signal $\log_2$ ratio that compares illuminated cultures with control cultures. No change from control cultures = 0. A twofold increase corresponds to a signal log ratio of 1.

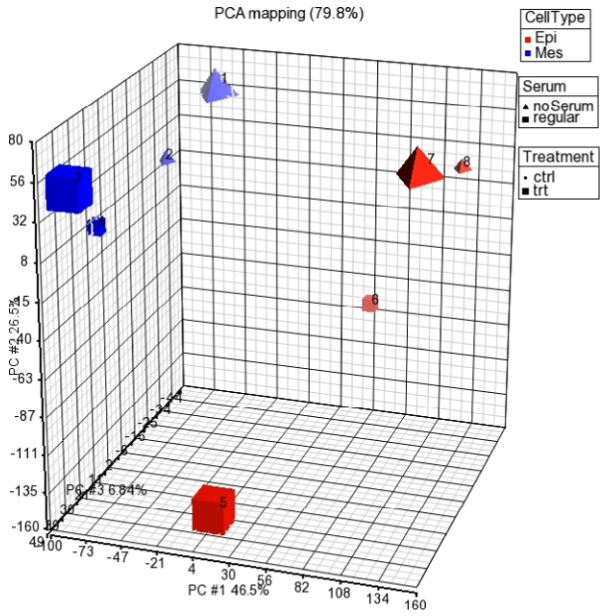

Fig. 7. Principle component analysis of epithelial (NHEK-Neo) vs. mesenchymal cell (hBMSC) cultures stimulated by LLLT under serum and serum-free conditions. Each axis measures variance between data points of gene sets identified by the Affymetrix HuEx 1.0 ST microarrays for the three different variables: mesenchymal vs. epithelial cell type, treated (IR 2.0 J/cm^2) vs. control and serum vs. serum-free media. Large distances between data points suggest dissimilarity (Partek Inc.).

phosphatase, type II collagen, fibronectin, and tenascin.

Microarrays suggest that keratinocytes and marrow stromal fibroblast (MSF) cells differ in their response to light

Principle component analysis (PCA mapping, Ingenuity software) compared the response of epithelial and mesenchymal cells to light under serum-containing and serum-free culture conditions. If the response to light was universal, regardless of cell type, then the treatment responses for the different cell types should converge. The PCA map summary (Fig. 7) suggested that the gene profiles for epithelial and mesenchymal cells, for both control and light-treated conditions, remained distinct despite common treatments. The treatment response could be large, but there was no convergence of data points for treated cells regardless of cell type or culture conditions. This data suggest a tissue-specific responses to the light stimulus.

Discussion

These findings of this study suggest that data from laser or light activation studies could be difficult to replicate whenever the experimental conditions vary in timing, distance from the light source, tissue type, energy density, wavelength of light, and cell type as each experimental condition produced a different panel of expressed genes. Our microarray data were supported by tight pairing of data points, quantitative PCR and protein arrays. To determine whether the changes were universal among cell types, we repeated the experiments comparing mesenchymal and epithelial cells. According to our comparative microarray analyses, the epithelial cells and mesenchymal cells expressed different profiles of genes. We did not see much overlap in the panel of activated genes between the two cell types. Although the capacity to respond to visible or infrared light via increased cytochrome-mediated ATP production (12, 13) may be present in all cells, there does not appear to be a common shared gene expression response to light between epithelial and mesenchymal cells. Observed differences could be due to inherent differences between an epithelial and a mesenchymal cell. From a clinical application point of view, light therapy might be exploited to target specific cell types as all cells will not be stimulated in the same manner (14).

The differential gene expression induced by light of different wavelengths and energy levels represents a powerful adjunctive tool for stem cell research. Stem cells may be considered a repository of different cellular signals involved in tissue repair that can be released at specific stages of activation, differentiation, and function (15). Depending on the stage of repair and the wavelength and dosage used, light could potentially stimulate the expression of sets of genes that activate stem cells, target a distant injury site though systemic effects (16), or potentiate and accelerate certain repair processes at the early immunomodulatory stage or at the late tissue remodeling stage. The VR and IR light switching of canonical and non-canonical pathways for

TGF-beta 1 raises the question of whether light might stress the cells (17, 18), thereby turning off canonical pathways and activating alternative pathways to achieve similar cell function. Light also activated cell proliferative pathways such as Akt 1 and therefore has additional risks and side effects. These functions are tightly regulated in development and tissue repair and are abnormally expressed in cancer cells (19, 20). The use of LLLT in human subjects carries the risk of activating the Akt 1 pathways expressed during oncogenesis (21). Our study did not test for return to baseline gene and protein expression following removal of the light stimulus, an important future experiment needed for the development of light-mediated activation of MSF cells.

Interestingly, TGF-beta 1 is a growth factor that can have multiple, even opposite, functions depending on the cell type and tissue (20, 22). TGF-beta 1 plays a role in bone homeostasis (20). Specifically, when activated by bone resorption it can promote migration of precursor cells and differentiation of cell phenotypes (22). The TGF-beta 1 pathway has been implicated in modulation of odontoblast differentiation by LLLT at wavelengths of 810 nm (23). This study differed from our work because of the longer light wavelength, repetitive treatments, high energy density (3 J/cm^2), and short time course. Our data showed that TGF-beta 1 expression was above control at 830 nm but that the maximal change was at 0.5 J/cm^2 for VR light at a wavelength of 633 nm. The exact conditions for exploiting TGF-beta 1 and Akt 1 responses need to be explored for different cell and tissue responses. The current study points to these two pathways as important gene networks to consider in developing future therapeutics.

If tooth movement can be thought of as a form of regional acceleratory phenomenon (24), then our findings support studies reporting that infra red light (830 nm) can upregulate RANKL and OPG synthesis and assist the initial resorptive phase of the tooth movement process by activating osteoclasts (25, 26). At this wavelength, RANKL, an activator of osteoclasts, was expressed in a dose–response curve on exposure to light energy whereas expression of OPG, its decoy receptor/inhibitor, remained unchanged. With exposure to the visible red wavelength (633 nm), the difference between the responses of RANKL and OPG were insignificant. In rat studies on tooth movement, similar LLLT responses in RANKL and OPG protein expression were reported by Fujita et al. (25). Thus, light-induced changes in the RANKL/OPG ratio could potentially mimic tooth movement and the osseous changes caused by injection of RANKL for accelerated tooth movement and of OPG for retention (27). In addition to RANKL upregulation at 830 nm, MMP10 was upregulated in a dose-dependent manner while TIMP 1, its inhibitor was unchanged. Randomized human clinical trials (9) appear to agree with the 830 nm wavelength as one wavelength for accelerating tooth movement.

There are inherent limitations in the use of microarray data. For example, microarray data are based on mRNA content and do not consider post-transcriptional regulation such as miRNA silencing, translation, post-translational modifications, secretion, synergistic protein functions, and intercellular cross-talk control of a particular gene. Such data also lack tissue context in terms of time, position and cell type interactions. Hence, interpretation of microarray data can produce an incomplete biological picture of how LLLT works in patients. In addition, a twofold screen for gene expression changes pre-supposes that nature works only with large changes in gene expression. It may be that tissue responses could be associated with smaller changes in gene expression. Our study generally corroborates a previous microarray study by Wu et al. (28) that describes the Akt 1 pathway as being a principle pathway that is activated by LLLT. An earlier study by Zhang (29) used H27 newborn foreskin fibroblast cells exposed to a LLLT energy density of 0.88 J/cm energy density, reported similar functional categories of genes activation as was reported here. The current study is one of the largest microarray experiments conducted to date for multiple conditions which included two wavelengths of light at four different energy densities. We will place our data in the Gene Expression Omnibus (GEO) public repository operated by the National Center for Biotechnology Informa-

tion. To further advance our understanding, we are presently conducting a time-dependent series of microarrays to capture the cascade effects occurring immediately after illumination and at time points within the first 24 hours. Functional assays are needed to confirm the mechanisms behind the TGF-beta 1 and Akt 1 pathways. Wang et al. (30) previously showed that there were time-dependent changes in cell proliferation and cell cycle-associated genes. Preliminary data showed that the expression panels of early vs. late gene expression were different. This implies that the differences between timing of treatment and collection of data may also contribute to the confusion when comparing data from different studies. Despite these concerns, use of LLLT offers the possibility of altering pathway responses in a dose-specific manner that can target particular cell types and tissues and is not limited by biological vectors and carriers. As a possible therapeutic approach, light exposure therefore represents a promising method for potentiating tissue responses, altering oncogenic pathways, and activating stem cell functions.

Conclusions

Changes in light wavelengths and energy densities can produce unique sets of deregulated genes that were identified by microarray analysis. Pathway analysis pointed to TGF-beta 1 in the visible red and Akt 1 in the infrared wavelengths as key pathways to study. TGF-beta protein arrays suggest switching from canonical to non-canonical TGF-beta pathways as the wavelength shifted from visible to infrared wavelengths. Microarrays suggest RANKL and MMP10 followed dose–response curves in the infrared region. Epithelial and mesenchymal cells respond differently to stimulation by light suggesting cell type-specific response were possible. These studies demonstrated differential gene expression due to changes in wavelengths, energy densities, and cell types were possible. These differences in gene expression could potentially be exploited for therapeutic purposes and help explain contradictory results in the literature when experimental conditions differ.

Clinical relevance

This study supports the use of low-level laser treatment (LLLT) as a method for stimulating distinct sets of genes in human marrow stromal fibroblast MSF cells that can change by altering the wavelength, energy density, cell type and timing of application. If the conditions are carefully chosen, there is potential for inducing gene expression changes that are favorable for different stages of orthodontic tooth movement. The observations from this study identified key pathways, candidate genes and different gene responses which explains how contradictory data can be reported when the experimental conditions differ.

Acknowledgements: This research was funded in part by departmental funds and by scholarships from the Chinese Government and Shandong University. The authors would like to express gratitude to Paul Matthews for building the LED arrays and optical engineering support and to Peter Brawn for donating the custom light units and for his encouragement and friendship.

References

1. Tortamano A, Lenzi DC, Haddad AC, Bottino MC, Dominguez GC, Vigorito JW. Low-level laser therapy for pain caused by placement of the first orthodontic arch wire: a randomized clinical trial. *Am J Orthod Dentofacial Orthop* 2009;136:662–7.
2. Tim CR, Pinto KN, Rossi BR, Fernandes K, Matsumoto MA, Parizotto NA, Rennó AC. Low-level laser therapy enhances the expression of osteogenic factors during bone repair in rats. *Lasers Med Sci* 2014;29:147–56.
3. Rochkind S, Geuna S, Shainberg A. Phototherapy and nerve injury: focus on muscle response. *Int Rev Neurobiol* 2013;109:99–109.
4. Gomes FV, Mayer L, Massotti FP, Baraldi CE, Ponzoni D, Webber JB, de Oliveira MG. Low-level laser therapy improves peri-implant bone formation: resonance frequency, electron microscopy, and stereology findings in a rabbit model. *Int J Oral Maxillofac Surg* 2014;pii:S0901-5027(14)00343-9.
5. Gkantidis N, Mistakidis I, Kouskoura T, Pandis N. Effectiveness of non-conventional methods for acceler-

ated orthodontic tooth movement: a systematic review and meta-analysis. *J Dent* 2014;42:1300–19.
6. Limpanichkul W, Godfrey K, Srisuk N, Rattanayatikul C. Effects of low-level laser therapy on the rate of orthodontic tooth movement. *Orthod Craniofacial Res* 2006;9: 38–43.
7. Colombo F, Neto Ade A, Sousa AP, Marchionni AM, Pinheiro AL, Reis SR. Effect of low-level laser therapy (λ 660 nm) on angiogenesis in wound healing: a immunohistochemical study in a rodent model. *Braz Dent J* 2013;24:308–12.
8. Barboza CA, Ginani F, Soares DM, Henriques AC, Freitas Rde A. Low-level laser irradiation induces in vitro proliferation of mesenchymal stem cells. *Einstein (Sao Paulo)* 2014;12:75–81.
9. Kau CH, Kantarci A, Shaughnessy T, Vachiramon A, Santiwong P, de la Fuente A, Skrenes D, Ma D, Brawn P. Photobiomodulation accelerates orthodontic alignment in the early phase of treatment. *Prog Orthod* 2013;14:30.
10. Zhang QZ, Su WR, Shi SH, Wilder-Smith P, Xiang AP, Wong A, Nguyen AL, Kwon CW, Le AD. Human gingiva-derived mesenchymal stem cells elicit polarization of m2 macrophages and enhance cutaneous wound healing. *Stem Cells* 2010;28:1856–68.
11. Yamaza T, Miura Y, Bi Y, Liu Y, Akiyama K, Sonoyama W, Patel V, Gutkind S, Young M, Gronthos S, Le A, Wang CY, Chen W, Shi S. Pharmacologic stem cell based intervention as a new approach to osteoporosis treatment in rodents. *PLoS ONE* 2008;3:e2615.
12. Oron U, Ilic S, De Taboada L, Streeter J. Ga-As (808 nm) laser irradiation enhances ATP production in human neuronal cells in culture. *Photomed Laser Surg* 2007;25:180–2.
13. Xuejuan G, Da X. Molecular mechanisms of cell proliferation induced by low power laser irradiation. *J Biomed Sci* 2009;16:4.
14. Mognato M, Squizzato F, Facchin F, Zaghetto L, Corti L. Cell growth modulation of human cells irradiated in vitro with low-level laser therapy. *Photomed Laser Surg* 2004;22:523–6.
15. Caplan AI, Correa D. The MSC: an injury drugstore. *Cell Stem Cell* 2011;9:11–15.
16. Tuby H, Maltz L, Oron U. Induction of autologous mesenchymal stem cells in the bone marrow by low-level laser therapy has profound beneficial effects on the infarcted rat heart. *Lasers Surg Med* 2011;43:401–9.
17. Akhurst RJ. The paradoxical TGF-β vasculopathies. *Nat Genet* 2012;44:838–9.
18. Coombe AR, Ho CT, Darendeliler MA, Hunter N, Philips JR, Chapple CC, Yum LW. The effects of low level laser irradiation on osteoblastic cells. *Clin Orthod Res* 2001;4:3–14.
19. Testa JR, Tsichlis PN. AKT signaling in normal and malignant cells. *Oncogene* 2005;24:7391–3.
20. Massagué J. TGFβ signalling in context. *Nat Rev Mol Cell Biol* 2012;13:616–30.
21. Sperandio FF, Giudice FS, Corrêa L, Pinto DS Jr, Hamblin MR, de Sousa SC. Low-level laser therapy can produce increased aggressiveness of dysplastic and oral cancer cell lines by modulation of Akt/mTOR signaling pathway. *J Biophotonics* 2013;6:839–47.
22. Tang Y, Wu X, Lei W, Pang L, Wan C, Shi Z, Zhao L, Nagy TR, Peng X, Hu J, Feng X, Van Hul W, Wan M, Cao X. TGF-beta 1-induced migration of bone mesenchymal stem cells couples bone resorption with formation. *Nat Med* 2009;15:757–65.
23. Arany PR, Cho A, Hunt TD, Sidhu G, Shin K, Hahm E, Huang GX, Weaver J, Chen AC, Padwa BL, Hamblin MR, Barcellos-Hoff MH, Kulkarni AB, J Mooney D. Photoactivation of endogenous latent transforming growth factor-β1 directs dental stem cell differentiation for regeneration. *Sci Transl Med* 2014;6:238.
24. Verna C, Zaffe D, Siciliani G. Histomorphometric study of bone reactions during orthodontic tooth movement in rats. *Bone* 1999;24:371–9.
25. Fujita S, Yamaguchi M, Utsunomiya T, Yamamoto H, Kasai K. Low-energy laser stimulates tooth movement velocity via expression of RANK and RANKL. *Orthod Craniofac Res* 2008;11:143–55.
26. Yamaguchi M. RANK/RANKL/OPG during orthodontic tooth movement. *Orthod Craniofac Res* 2009;12:113–19.
27. Hudson JB, Hatch N, Hayami T, Shin JM, Stolina M, Kostenuik PJ, Kapila S. Local delivery of recombinant osteoprotegerin enhances post-orthodontic tooth stability. *Calcif Tissue Int* 2012;90:330–42.
28. Wu YH, Wang J, Gong DX, Gu HY, Hu SS, Zhang H. Effects of low-level laser irradiation on mesenchymal stem cell proliferation: a microarray analysis. *Lasers Med Sci* 2012;27:509–19.
29. Zhang Y, Song S, Fong CC, Tsang CH, Yang Z, Yang M. cDNA microarray analysis of gene expression profiles in human fibroblast cells irradiated with red light. *J Invest Dermatol* 2003;120:849–57.
30. Wang J, Huang W, Wu Y, Hou J, Nie Y, Gu H, Li J, Hu S, Zhang H. MicroRNA-193 pro-proliferation effects for bone mesenchymal stem cells after low-level laser irradiation treatment through inhibitor of growth family, member 5. *Stem Cells Dev* 2012;21:2508–19.